

Versatile tape-drive for high-repetition rate laser-driven proton acceleration

N. Xu,¹ M. J. V. Streeter,² O. C. Ettlinger,¹ M. Balcazar,³ M. Borghesi,² N. Bourgeois,⁴ C. B. Curry,⁵ S. Dann,⁴ S. Dilorio,³ N. P. Dover,¹ T. Dzelzanis,⁴ V. Istoksaia,⁶ M. Gauthier,⁵ L. Giuffrida,⁶ G. D. Glenn,⁵ S. H. Glenzer,⁵ R. Gray,⁷ A. Hamad,⁴ G. S. Hicks,¹ M. King,⁷ B. Loughran,² D. Margarone,² O. McCusker,² P. McKenna,⁷ C. Parisuaña,⁵ D. Symes,⁴ A. G. R. Thomas,³ F. Treffert,⁵ C. A. J. Palmer,² and Z. Najmudin¹

¹*Blackett Laboratory, Imperial College London, South Kensington Campus, London, U. K.*

²*School of Maths and Physics, Queen's University Belfast, University Road, Belfast, N. Ireland, U. K.*

³*Center for Ultrafast Optical Science, University of Michigan Engineering, 1221 Beal Ave., Ann Arbor, Michigan, U. S. A.*

⁴*Central Laser Facility, STFC Rutherford Appleton Laboratory, Harwell Campus, Didcot, U. K.*

⁵*SLAC National Accelerator Laboratory, 2575 Sand Hill Road, Menlo Park, California, U. S. A.*

⁶*ELI Beamlines, Za Radnicí 835, 252 41 Dolní Břežany, Czech Republic*

⁷*Department of Physics, University of Strathclyde, 16 Richmond Street, Glasgow, U. K.*

(*Correspondence email address: c.palmer@qub.ac.uk, n.xu19@imperial.ac.uk)

(Dated: 4 August 2022)

We present the development and characterisation of a high stability, multi-material, multi-thickness, variable speed tape-drive target, suitable for laser-driven proton acceleration at repetition rates of up to 100 Hz with enhanced diagnostics access. The tape surface position was measured to be stable on the sub-micron scale. This is therefore compatible with high numerical aperture focusing geometries, as is required to achieve relativistic intensity interactions with the mJ-laser-pulse-energies available in current and near-future multi-Hz lasers. The target was continuously used in a recent experiment for 70,000 shots without intervention by the experimental team with the exception of periodic replacement of the tape spools. This tape-drive provides a robust target system for the generation and study of high-repetition rate ion beams using the next generation of high-power laser systems thereby also enabling wider adoption of laser-driven proton sources for applications.

I. INTRODUCTION:

The interaction of high-irradiance lasers ($> 10^{18} \text{ Wcm}^{-2} \mu\text{m}^2$) and micron scale target foils has been demonstrated to provide a robust source of directional proton beams with energies of tens of MeV¹. These are accelerated via the well-studied sheath acceleration mechanism². This makes them very attractive for a variety of applications including time-resolved deflectometry measurements of electric and magnetic fields in dense plasmas³, the generation of medical isotopes⁴ and materials testing via proton-induced x-ray emission⁵ amongst others. To date a key impediment to the wider adoption of these accelerators has been the low average flux due to laser shot rates significantly below 1 Hz.

In the last decade joule-class, multi-Hz repetition rate lasers suitable for laser-driven proton acceleration have become available⁶. This enables the production of MeV proton beams at up to 10 Hz, and near-future laser systems will likely extend this to 100 Hz⁷ and beyond. Adaptation of the targets to replenish the target foils, which are destroyed during the acceleration process, is now a crucial area of development.

There are several key challenges to the development of multi-Hz targetry for laser-driven proton acceleration. Firstly, long periods of operation with hundreds to thousands of shots, required of a user facility, will consume large amount of target material. This limits the utility of raster targets which have foils mounted on a grid or disk turret type targets⁸ that are

translated or rotated to access a fresh region of foil for the next shot. Tape-drives can provide a compact alternative, with sufficient fresh tape for several thousand shots being constantly supplied from one spool and removed by another. Most importantly, refreshing targets (raster or tape-drive) in under 10 milliseconds cycle time has proven to be challenging, mainly due to positional instability.

The peak particle energies produced in laser-solid interactions nominally scale with the laser intensity I_0 to some power ($I_0^{1/2}$ for sheath acceleration⁹) and so tight focusing is generally desirable. As this then results in a short Rayleigh length, often less than $10 \mu\text{m}$, the tolerance for target positioning accuracy is correspondingly small. This scale of interaction tolerance not only limits the target delivery system to have low intrinsic positioning jitter at high operating speed, but also requires the body of the tape drive and link to further mounting structures to remain stable, having low long term thermal drift and low geometric drift due to internal stress characteristics. In addition, long periods of operation will consume large amount of target material. Rapid reloading of target material with high repeatability is therefore required. Kinematic coupling of various target components (e.g. tape drive to mount), or use of precision alignment dowels, will reduce or eliminate additional alignment after target reload, or other operation involving tape-drive removal from its mounting within the interaction vacuum chamber.

Long timescale operation over days and weeks will also

produce significant amounts of debris. The problem of debris is compounded by the issue of tight focusing, which requires the final focusing optic (often one of the most expensive components of the system) to be in close proximity to the debris source. Studies of the characterisation and management of debris (e.g. angular variation of debris emission, the effectiveness of thin pellicle shields for high value optics) are underway but beyond the scope of this work.

Here, we report on the development and characterisation of a tape-drive target with sub-micron positional stability capable of 100 Hz operation. This tape-drive was demonstrated in a high-intensity laser-plasma experiment, accelerating proton beams to a few MeV at up to 5 Hz, which was only limited by the operation rate of the laser.

II. TAPE-DRIVE TARGET DESIGN CONSIDERATIONS

State of the art high repetition rate (100Hz - 1kHz) laser systems generate pulses with < 1 J of energy and so the laser focusing optic must have an f -number of $N \lesssim 3$, to achieve relativistic intensities. This corresponds to a diffraction limited focal spot radius ($1/e^2$) of $1.5\mu\text{m}$ and a Rayleigh range of $18\mu\text{m}$. However, most 100 Hz class lasers will operate at $\ll 100$ mJ level, further reduce Rayleigh range due to tighter focusing optics. A tape-drive target will therefore require better than $5\mu\text{m}$ RMS positional jitter. In addition, better than $2\mu\text{m}$ (scale of typical high rep-rate drive laser focusing optics Rayleigh length) long-term structural thermal growth relative to the mounting point is required to achieve reasonably stable beam generation over long operation periods. This poses challenges including choice of tape material and tape drive design to maintain high stiffness over a large tape span, and symmetrical thermal design to reduce the effect of motor warm-up induced mid-term target position drift. Material stress releasing should also be considered with special machining procedures combined with heat treating to ensure long term geometric accuracy under thermal cycle and vibration. Other challenges including EMP-resistance and radiation hardening of the drive electronics and power supply should be considered if budget permits. These latter constraints usually result in very limited choices of drives from a small selection of space-rated hardware, which is often obsolete. However, these issues (EMP and radiation hardening) can also be mitigated with circuit board layout, feed-thru filtering, and additional enclosure shielding.

Other research groups have published different straight forward tape-drive design approaches such as using plastic guide rollers and spring tensioning devices to guide tape around a flat aluminium structural plate to achieve good $1\mu\text{m}$ RMS short-term (10 seconds) positional stability for use with Joule-class multi-Hz laser systems¹⁰, however such approach will be unsuitable at high repetition rate due to feedback loop response time and unnecessary in added complexity compare to open loop design. Other commonly used designs for higher repetition rate (10Hz) tape-drives utilise stationary guide pins (mostly made from tungsten carbide with a lapped finish surface or occasionally a steel / stainless cylindrical pin)¹¹. These

designs are commonly reported with high surface positional error and jitters ($> 10\mu\text{m}$ RMS). To the knowledge of the authors, no long-term ($> 100\text{s}$) thermal and structural drift characterisation have been published.

The conclusion of this is that selection of the motors used for the transfer of the tape between spools and how this is combined with the target frame is crucial for long-term target stability.

A. Motor selection

Commonly, in precision motion control systems, closed-loop encoder feedback servo motors are used. A modern servo motor usually consist of a brushless DC motor with a field oriented control motor driver, and different feedback loop running a realtime Digital Signal Processor (DSP) in order to realize encoder positional feedback. Most importantly, this provides the user with a constant rotation speed regardless of load variation and other disturbance. The servo motor can also be used in a constant torque feedback mode, providing constant tape tensioning regardless of tape surface linear speed, and tape material inconsistencies.

However, these motors suffer from a number of issues. Due to the lack of availability of ultra-high vacuum (UHV) compatible servo motors, standard motors are frequently used. These often overheat; exude undesirable vacuum contaminants depending on material and lubrication choice; and out-gas due to trapped volumes in the sealed shaft optical encoder, which cannot be easily modified to be vacuum compatible. In addition, a commercial off-the-shelf servo motor is not hardened to the high levels of EMP and radiation found in the near vicinity of a high-intensity laser-solid interactions. The encoder readout unit can easily be damaged from this EMP. The motor winding insulation material can be radiation damaged, causing it to crumble and fail through electrical shorts. It is also common for the motors to require many differential signaling twisted pairs for good common mode rejection of coupled electromagnetic interference which make them hard to interface out from the vacuum chamber for remote closed loop motor driving. Some servo motors provide a stepper-like interface which has a built-in servo driver. Although this enables electrical feed-through with a low pin count connector, it can very easily overheat due to the compact high-power electronics location, which is in close proximity to the heat-generating motor winding.

One other common type of motor used in the motion control industry is the hybrid stepper motors. Many commercial variants of stepper motor are available off-the-shelf, offering proven radiation hardening and UHV compatibility. These are also available at affordable prices due to their common use in the semiconductor and space industries. A stepper motor has much finer pole spacing compared to servo motors. Therefore, when running in synchronous mode without any encoder feedback, it can achieve good angular resolution without load (0.9° for majority of fine pole stepper, 1.8° for high-torque, high-speed steppers). The relatively loose angular positioning resolution (between stepper poles, equivalent to ~ 1 mm

with commonly used drive spool diameter) needed for a high repetition-rate tape-drive is due to other limiting factors such as tape material inhomogeneity. A microstep-capable stepper motor driver can provide more than enough angular resolution to ensure smooth operation. Due to the same material limitations, other methods such as registration sprocket and fiducial markers, will be required to enable repeatable absolute positioning accuracy across many metres of tape.

Brushed DC motors are traditionally used as a pseudo-constant torque device in tape-drive construction within many fields, such as commercial off-the-shelf magnetic tape audio reproduction devices and data recording devices where it is both used as driver and for feed/take-up spool tensioning to prevent tape entanglement. When operating at low speeds, where motor back EMF can be ignored, regulated DC source driven brushed motors can adapt to time varying loads without any encoder feedback. The brushed motor offers robust torque control regardless of EMP, as they do not require any digital closed-loop feedback. However, despite this benefit and proven readiness, through its use in fields of tape manipulation such as audio and video recording devices, graphite brush dust and many other non-vacuum compatible properties result in these not being a viable option to drive tape-drives for laser-plasma experiments.

Having reviewed the commercially available tape-drives outlined above, it was concluded that the stepper motor offers both low-cost, easy-implementation and -interfacing for a high-intensity laser solid experiment operating at up to 100 Hz in vacuum.

B. Motor driver selection

Stepper motors unlike brushed DC motors, need multiple phases to drive. Therefore, at least a traditional H-bridge commanded by micro-controller, or more commonly nowadays a dedicated stepper driver chipset, is needed. In the process of selecting a stepper driver, we can benefit from the rapidly growing market of consumer indoor 3D-printing devices, which has driven the recent development of many low audible noise stepper drivers. These stepper drivers produce a finer approximation of a sine wave phase current using a more accurate and higher sample rate sine-wave subdivision method compare to traditional stepper driver chipset. Traditionally, a A4988 chipset-based microstepping driver produces significant harmonic distortion as well as modulation frequency induced vibration, which is unsuitable for low jitter operation as the motor is rigidly mounted onto the tape-drive frame¹². The motor driver choice of the TMC2208 chipset is determined by comparing different commercial off-the-shelf stepper motor micro-stepping application-specific integrated circuits (ASIC). This chipset provides minimal drive waveform total harmonic distortion, high sinusoidal pulse width modulation (SPWM) carrier frequency, as well as low timing jitter induced motor vibration. To reduce heating during the spooling operation, the stepper motor driver is tuned with minimal drive current while maintaining adequate torque. Disabling DC holding mode, which, when enabled, typically pro-

vides locking torque to prevent tape from un-spooling under tension, further reduces motor heating. In theory, this will sacrifice stability on startup when there is a quick change in torque. However, due to the iron core having a significant cogging effect, which provides enough braking torque even without power, the drive structure stays steady from cold startup (in the previously operated tape tension state) to optimum operating condition within 0.1 s without sudden variation from start-up torque difference (figure 1). This eliminates sudden straining of the tape-drive structure.

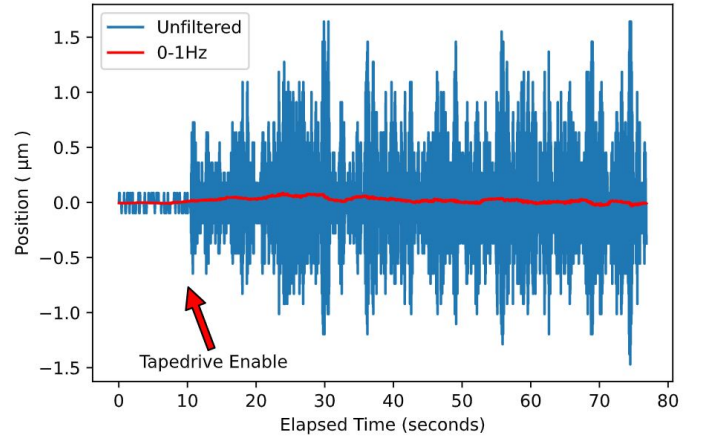


FIG. 1. Position measurements of target tape using the CHRocadile instrument illustrating the vibrations associated with start-up of the tape drive. The instrument background and intrinsic breadboard vibration can be observed for 'elapsed times' less than 10 seconds. Following start-up the position of the tape surface as it spools past the detector is provided for just over 1 minute following start-up. For the whole measurement time-period the instantaneous surface position measured with a temporal sampling width of 15 microseconds is provided in blue together with the low-pass filtered signal with a cut-off of 1 Hz to demonstrate long term drifting behaviour.

C. Modal analysis and motor tuning

Modal analysis provides frequency domain information in response to excitation as well as allowing resonance transmissibility to be calculated. This analysis highlights resonance frequencies and their quality factor (similar to gain bandwidth). Modal analysis with finite element method was performed with Fusion 360's parametric modelling and finite-element analysis package to provide guidance on the structural design, with a reduced complexity representation of actual mass distribution to enable rapid computing cycle. The resulting displacements of tape drive components for one of the resonance modes are illustrated in figure 2.

In particular, the design must avoid the common 50 Hz excitation source frequency such as mains powered devices (which in some rare occasions may be 60 Hz), as well as 90 Hz if using modern dry roots pump with internal variable frequency drive. Pump vibration and their harmonics, especially second harmonic (100 Hz / 120 Hz / 180 Hz), were

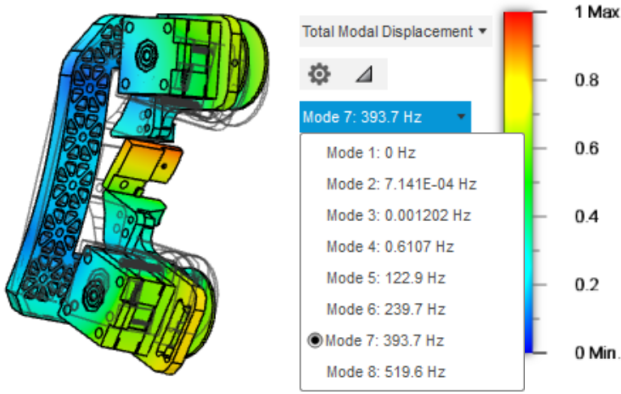


FIG. 2. Finite element modal response analysis of the tape drive illustrating the positional displacement of the tape drive components fixed to a rigid breadboard associated with resonant oscillations of the tape drive at 393.7 Hz. The resonant frequency modes of the structure are listed.

avoided during design and finite element analysis iteration process. The motor driver current modulation carrier frequency, which is normally sufficiently high so as to not excite vibration modes with enough quality factor to cause problems, should also be avoided if possible.

Motor spooling speed induced vibrations of various speed typically spanning from 0.1 - 10Hz due to motor rotor and tape reel assembly imbalance provide another source of vibrations. These should be reduced with dynamic balancing. Alternatively, tape speed dithering (intentionally applied form of noise with certain power spectral density avoiding resonance) can be utilised if the off-the-shelf stepper motor cannot withstand disassembly to achieve mechanical balancing.

Careful consideration of these resonance during design can help to mitigate target instability. Increased structural stiffness will reduce the absolute amplitude for a given excitation and material damping property. A weight reduction grid pattern was added to the considered tape-drive mount in order to tune the structural response without significant reduction in stiffness. Such an isogrid-like pattern, with small feature size and high aspect ratio, requires modern manufacturing methods in order to minimize excessive machining stress which can be imposed onto the material. This stress would cause structural warping on the micron scale over time, and over repeated thermal cycles. Other strategies such as active dampening by inertia reference measuring unit containing low angular random walk gyroscope and large dynamic range accelerometer could be useful but alone will cost significantly more than most experimental setup, therefore not discussed here.

It is not possible to isolate the tape-drive from all vibrations and so, to maximise tape stability, it is also important to consider mechanisms to improve the damping quality of the entire target setup, including both the translation stages used to adjust the position of the target in the chamber and the attached tape-drive, as a complete system, in addition to mechanisms to

rapidly dissipate any vibrations. Translation stages with precision ground or scraped hydrostatic guide-ways¹³ can dissipate vibrations significantly faster than ball or cross roller bearing linear rails, and therefore should be used with vacuum compatible oil if budget permits. In the future, further improvements on damping quality can be achieved with the addition of a vacuum compatible epoxy-sand mixture, or other types of epoxy granite¹⁴.

D. Manufacturing considerations

As discussed previously, the manufacture process can influence the stability of the tape-drive through the induction of material stress responses that manifest through deformation of the tape drive over time. Therefore, it is vital to consider and adapt the manufacturing approach appropriately. For example, a lapped flute end-mill should be used during machining, in order to avoid excessive surface stress induced from rubbing, which will impact long term geometric stability.

In some cases, to ensure vacuum cleanliness, all material should ideally be machined completely dry without cutting oil or water soluble coolant. For deep pocket and high aspect ratio machining, minimal quantity lubrication mist (MQL) of ethanol can be used to avoid chip welding. In addition, brass alloys containing zinc should ideally be avoided due to their high vapour pressure even at room temperature. Often, this latter condition can be relaxed as the typical vacuum levels for laser-plasma particle accelerators are on the order of 1×10^{-6} mbar as opposed to ultra-high-vacuum required by radio-frequency accelerators.

Tape stability is improved with the addition of a tape support plate, over which the tape is pulled. Design and attachment of this support should be such that restrictions on diagnostic viewing angle are minimised. For maximum flexibility, the tape support plate should be removable to provide full diagnostic access. However, this access is at the cost of reduced long term geometric stability performance as any structural change will directly impact tape position. The support plate should be fixed to a position that has relatively short accumulated distance from the tape-drive support, as this mitigates the impact of thermal growth. Instead of total removal of the tape support, the support can also be customised, for example providing a narrow channel feature for shallow off-axis diagnostics as visible in figure 6. Sharp corner grooves should be avoided to prevent stress concentration. While manufacturing of this access cut-out would ideally utilise 5-axis machining, it can be achieved by traditional filing as was the case for the example shown.

Tape guiding and support plate surfaces that come into direct contact with the tape should be mirror polished, as any surface imperfection will be directly imprinted onto the tape, thus affecting stability. This can be easily achieved by hand lapping, with a precision flat ground stone, or a diamond charged lapping plate. There is no benefit or requirement for other methods such as single point diamond turning or milling with a monocrystalline diamond tool, as absolute global flatness over the whole guide plate is not important since tape

internal stress differences as well as surface roughness, dominate positional inaccuracy in the scale of the laser focal spot size.

III. CHARACTERISING TAPE-DRIVE PERFORMANCE

Traditional contact metrology setups, such as dial test indicators, Linear Variable Differential Transformer (LVDT), and scanning Coordinate Measuring Machine (CMM) probes exert too much force onto the thin unsupported tape. They would deform the surface preventing accurate measurement during the highly dynamic tape spooling process. They also have limited bandwidth due to probe inertia.

Hetrodyne interferometers, such as the commercial Renishaw XL-80, can in theory provide measurements of surface stability using a direct surface reflection at 50 kHz without the need for a retro-reflector cube. Interferometry has the potential benefit over other methods of long distances (a few metres) between the probe optics and interaction area (tape surface) which can allow in-situ diagnosis of tape position during experiments. The long stand-off distance is desirable as it minimises the solid angle occupied by the diagnostic and prevents the diagnostic from blocking access for other diagnostics. The distance also enhances expensive optic survivability under a potentially heavy debris load. However, a Renishaw XL-80, tested with a diagnostic aperture at approximately 2 m from the tape, was limited by signal-to-noise ratio. This occurred, in this case, due to the combination of long stand-off distance of the detector and poor reflection of the probing laser from the semi-transparent, plastic tape. This can be due to photon loss to transmission and poor surface quality of the tape, both leading to energy loss in the diagnostic collection angle. A more suitable inteferometer for long-distance remote surface monitoring would utilise a high power narrow line width fiber laser as a reference source, but this has yet to be done.

A confocal white light probe, such as the commercial Precitec CHRcodile, provides high resolution sub-micron ranging albeit with relatively short working distance (< 5 mm to achieve high enough spacial resolution). This is unsuitable for most on-shot diagnostics as it will block the drive laser (as well as other diagnostic lines). Also, its close proximity to the tape surface will lead to debris accumulation on the first optic of the probe head. However, for off-line stability measurements the Precitec CHRcodile has shown good performance, with negligible noise level (significantly lower than $f/1$ Rayleigh range). It also requires no major alignment during setup which is useful during tape-drive characterisation and troubleshooting, and is small enough for in-situ measurements which capture the stability of the complete tape-drive system including translation stages. Its fast update rate reliably reaches 50 kHz with dark or transparent tape targets. This enables frequency domain analysis using fast Fourier transforms with high enough Nyquist bandwidth to provide useful iteration feedback on structural designs.

Direct off-axis imaging with a long working-distance objective or a laser parallax linear sensor requires little spe-

cialised hardware and can be flexibly adapted to the experimental setup. However, standard scientific cameras cannot provide high enough frame rates to diagnose most vibration and jitter problems. This method has been shown in same experimental setup with confocal white light probe to produce significantly underestimated vibration amplitude in comparison with a white light confocal probe, as it results in a blurry image and averaged out position with millisecond exposure time. Alternatively, more advanced cameras combined with strobe coaxial illumination can provide short exposures without motion blurring. However, they often run with sub-Nyquist sampling frequencies for commonly seen structural and motor vibrations. This makes the results hard to interpret, sometimes providing misleadingly low jitter information while other methods with more bandwidth shows significantly higher jitter distance.

Optical CMM and MEMS atomic force microscope can provide high line-frame rates as well as comparable 2D frame rate to an imaging camera. However, these devices are significantly more expensive than the previously discussed methods and cannot be used inside the vacuum since the MEMS probes require an environmental pressure close to 1bar to operate, and optical CMM does not work under vacuum due to its air-bearing. Although not suitable for in-situ tape stability measurements, optical CMM can be used to provide measurements of surface roughness which, as was discussed earlier, can influence the effectiveness of other characterisation techniques. Surface roughness of the tape used for the demonstration studies contained within this paper, indicated a 'bubble' structure on thin (12.7 micron) Kapton tape (figure 4).

As can be seen from the previous discussion, in-situ tape measurements present a particular challenge due to the high value of space surrounding the interaction. However, due to the importance of target position to the on-target intensity and interaction dynamics, it is vital to have some in-situ, and preferably on-shot, measurement of target position. In the absence of a high-power-laser-based interferometer, it is often necessary to resort to a high numerical aperture image relay to image non-specularly scattered light from target. This can provide imaging with a few micron resolution depending on the imaging system. Such as system was employed to measure the on-shot stability of the tape-drive presented here. However, it is important to note that these measurements were performed with instrument noise significantly above tape drive positional jitter. The light from laser scatter and plasma self-emission at the target surface during the interaction was collected along an axis perpendicular to the laser propagation direction and imaged. However difference in per-shot laser energy generated different plasma plume sizes which limited the accuracy in centroid finding. While the resolution of the on-shot diagnostic was low (worse than $50\mu\text{m}$) in comparison to the Precitec CHRcodile, which was used for off-line stability measurement, it enabled the long term position of the target to be tracked. This was particularly important due to occasional shifts in tape position greater than the Rayleigh length, due to translation stage cross roller bearing guide slop been taken out suddenly from tape-drive or environment vibrations.

IV. HIGH-STABILITY TAPE DRIVE DESIGN AND CHARACTERISATION

A tape-drive with low size, weight, and power, as well as cost was designed, and constructed, based on the considerations outlined in the previous sections. The build material was chosen only to survive prolonged high vacuum exposure, instead of any consideration of out-gassing level due to cost constraints. Stepper motors were used to provide remote spooling and rewinding capabilities, and servo driven brake shoes were used to provide field programmable tensioning. The tape drive hardware (primarily the spools) could be rapidly swapped to enable both commonly available tape width options of 12.7mm and 25.4mm. Two rigid, hand lapped brass guide structures provided the primary tape support, while a stabilising plate was added between two supports to reduce tape inhomogeneity induced surface fluctuation around interaction area at a shallow angle, to further improve performance. The tape drive design is highly modular and these support plates can be easily removed for better diagnostic access. The tape supply and take-up wheel assembly total indicator runout (TIR, eccentricity measured with dial test indicator) was specially matched to the receiving motor shaft to minimise stepper motor shaft runout. This further reduces torque ripple induced structural deflection jitter due to eccentricity of the rotating elements.

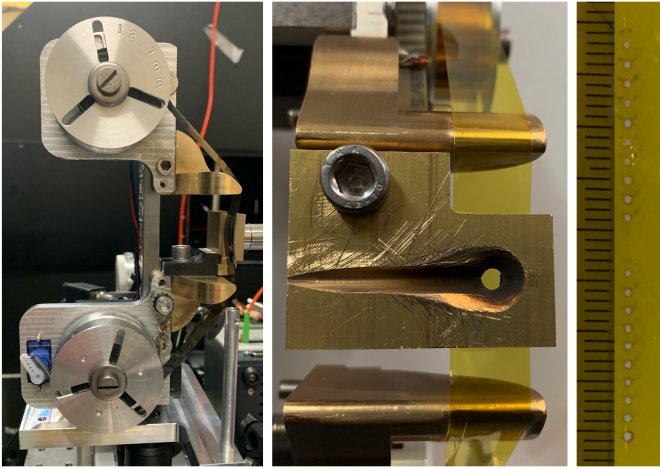


FIG. 3. Side-on photograph of the tape-drive showing the upper and lower spools as well as the brass frame which acts to support the tape at the interaction point for increased stability (left). Face-on photograph of the tape-drive zoomed in on the interaction point. This shows the transparent Kapton tape running vertically on the brass supports. The interaction point is at the centre of the hole in the brass support with the long groove to the left cut-away to provide improved diagnostic access from a shallow viewing angle for the on-shot target monitor (centre). (right) Photograph of tape after it has been shot with 400 mJ on target laser energy which produces <1 mm diameter holes. The black markers along the left of the tape are spaced by 1 mm.

In order to characterise the stability of the tape drive during spooling, a Precitec CHRocodile was used. This commercial

white light system has a noise floor of less than $0.1 \mu\text{m}$ and has a 66 kHz refresh rate. This makes it able to resolve high frequency movement of the tape.

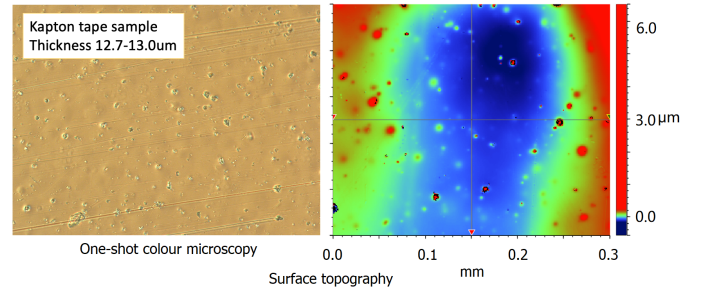


FIG. 4. Optical surface profiling of the $12.7 \mu\text{m}$ Kapton tape using optical coordinate-measuring machine (CMM), showing commonly found 'bubble' defect visible as dark-spots in the left image. Note that the lack of global flatness in the right image is an artifact of the measuring state (without tension)

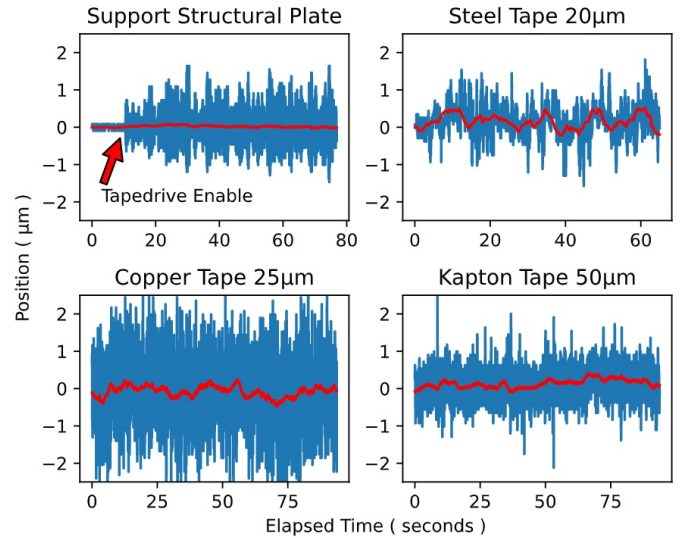


FIG. 5. Tape material positional jitter measured using the Precitec CHRocodile for over 1 minute ($> 60,000$ shot at 100 Hz) for different materials. The blue line provides the measurement with a temporal sampling period of 15 microseconds with high frequency changes attributed to tape surface roughness. The low (< 1 Hz) frequency movement, which better represents the tape motion, is shown with the red line.

Multiple materials, including steel, copper and Kapton, with different thickness from $13 \mu\text{m}$ to $50 \mu\text{m}$ were tested. The steel tape has a high modulus of elasticity. It therefore retained a non-flat shape locally and was subject to low frequency noise compare to the copper tape from which the surface roughness led to noisy data. Of these, the Kapton tape was the one that was predominately employed during the demonstration experiments. This is due to the availability of two thickness options including the thinnest of $12.7 \mu\text{m}$ which was most suitable for the low (100 mJ) energies of the driving laser pulses. CMM imaging of these tapes showed the pres-

ence of surface defects, with bubbles and indentations (figure 4). These lead to the small amplitude, high-frequency content of recorded tape-drive position, as the features pass through the Precitec CHRcodile field of view. An example of the Precitec CHRcodile trace measured over several minutes is presented in figure 5. These indicate that, aside from this high frequency noise, the motion of the tape is small ($< 2 \mu\text{m}$) with below resolution thermal drift over the several minutes operation periods. Similar behaviour is observed when the tape drive is run at different linear spooling speeds (corresponding to 25 - 100Hz operation at 1mm shot spacing, 0.1m/s linear tape speed). See table I for peak to peak and rms jitter from the different tape speeds.

	Kapton 50um	Kapton 12um	Steel	Copper
RMS error (micron)	0.28	1.11	0.49	0.92
Pk-pk error (micron)	3.48	7.05	3.39	6.13

TABLE I. Measured surface positional jitter with different tape material, 50um Kapton tape with best surface roughness shows 0.28um RMS tapedrive performance, the lack of better (ideally 10nm Ra roughness) surface quality sample limited true tapedrive performance characterization

V. TAPE-DRIVE PERFORMANCE IN REAL LASER-PLASMA INTERACTION ENVIRONMENT

The tape-drive was evaluated using the Gemini TA2 facility based at the Central Laser Facility of the Rutherford Appleton Laboratory. A laser driver operating at relativistic intensities ($4 \times 10^{19} \text{ W/cm}^2$), with up 400 mJ focused on to target with a short focal length off-axis parabolic mirror ($f/2.5$) and 1-5 Hz repetition rate, was used to generate MeV electron beams and proton beams, and evaluate tape-drive performance in an intense EMP and radiation environment.

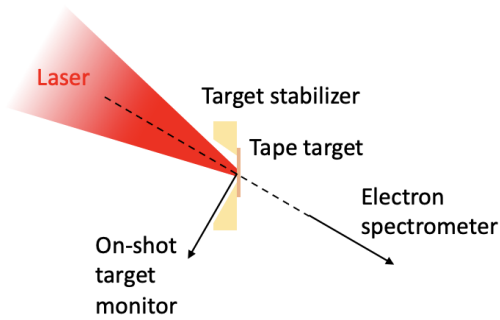


FIG. 6. On-shot tape position was monitored by imaging non-specular laser scatter and plasma self-emission at the laser fundamental and second harmonic, collected perpendicular to the axis of laser propagation.

The energy spectra of electron beams generated by the laser-tape interaction were characterised using a permanent magnet (150 mT) spectrometer with Lanex screen detector positioned at 24 cm from the interaction point, behind the target

along the axis of drive laser propagation (figure 6). Scanning of the tape-drive position relative to the static laser focus was achieved using a motorized XYZ stage. For these scans, data was recorded in bursts of 5 shots (each shot acquired independently) at 1 Hz for each target position before the target was shifted to a new z position with z aligned with the target surface normal. Note that due to the 30° laser angle of incidence at the target surface, the z -distances given correspond to the distance along the laser propagation axis multiplied by 0.87.

Figure 7 illustrates the burst averaged electron spectrum across a target position scan during which the target ($12.7 \mu\text{m}$ thick Kapton tape) was moved along the target surface normal in steps of $23 \mu\text{m}$. As expected, this indicates both increasing electron flux and maximum energy as the target position approaches best focus and correspondingly the highest laser intensities. This scan of 100 shots was acquired in approximately 3 minutes.

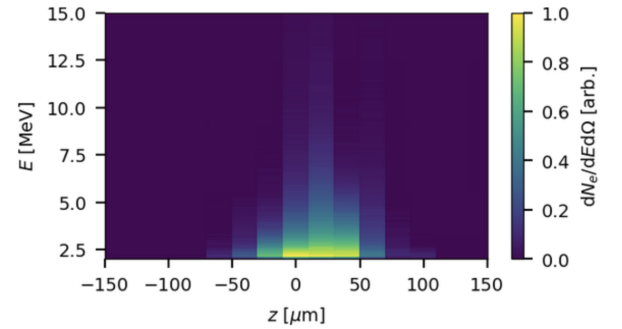


FIG. 7. Waterfall plot of the normalised forward propagating hot electron spectrum as tape-drive position is scanned through the laser focus. Negative values of z correspond to arrival of the laser pulse at the tape surface before the laser has reached best focus. Each vertical strip corresponds to the average electron spectrum retrieved from a burst of 5 shots at the recorded z position which was incremented in steps of $23 \mu\text{m}$ between bursts.

Due to the short focal length of the focusing optic used, the target positional stability is very critical. The distance over which the laser intensity drops by a factor of 2 in comparison with the best focus, the Rayleigh range, is $15 \mu\text{m}$. Despite the high short-term stability of the tape-drive, demonstrated through the measurements presented in figure 8, long-term stability across many hours and different days is required for ease of use. Changes in the relative position of the tape and motorised stage were addressed using an on-shot measurement of target position. Here, non-specular laser scatter and plasma self emission, at the laser fundamental and second harmonic, generated at the target surface were captured by an imaging line positioned perpendicular to the laser propagation axis and re-imaged onto a single shot focal-plane array (figure 6) as mentioned previously. The mapping of reflective surface position to the image plane of the diagnostic was characterised using non-specular scattered light at laser energies below the tape damage threshold collected as the static tape was driven through the diagnostic field of view. For both the characterisation and on-shot position extraction the image centroid was

used to retrieve the tape position and hence deduce the positional offset of tape-drive positioning linear slide. Due to limitations in the resolution of the diagnostic, and particularly due to the extension of the plasma spatial formation, on-shot target position measured using this technique is not as accurate as the previously discussed white light confocal method. Nevertheless this data was used to document tape position and monitor any unexpected changes indicative of a relative shift between tape and drive.

Throughout the experiment, the tape target was used for close to 70,000 laser shots. No operation difference was observed during this time indicating no degradation in tape-drive performance across the experiment.

VI. CONCLUSION

A sub-micron RMS jitter, multi-material, multi-thickness, variable speed tape-drive target capable of operating at up to 100 Hz was designed and constructed following detailed analysis of factors influencing tape short and long-term positional stability. This was demonstrated to have stability $< 1 \mu\text{m}$ over 1.5 minutes at 100Hz target refresh rate (only limited by available Kapton tape length). The technology of this tape drive was proven through its deployment within a multi-Hz, high-intensity laser-solid interaction experiment using a 400 mJ, 30 fs drive laser and short ($f/2$) focusing optic. The tape-drive operated reliably over more than 70,000 shots without any user intervention with the exception of replacement of the tape spools every few thousand shots.

Future developments of this target platform including further miniaturisation, larger tape capacity, and improved vacuum compatibility. EMP and radiation hardening hardware will also be investigated. Real-world ion acceleration performance with 100 Hz drive laser will be performed once laser source become available.

ACKNOWLEDGMENTS

Special thanks goes to the staff at the Central laser facility who provided laser operational support, mechanical and electrical support, computational and administrative support throughout the 5 months of the experiment.

We acknowledge funding from UK STFC, grant numbers: ST/P002021/1 and ST/V001639/1, U.S. DOE Office of Science, Fusion Energy Sciences under FWP No. 100182, and in part by the National Science Foundation under Grant No. 1903414. G.D.G. acknowledges support from the DOE NNSA SSGF program under DE-NA0003960.

DATA AVAILABILITY STATEMENT

The data that support the findings of this study are available from the corresponding author upon reasonable request.

¹H. Daido, M. Nishiuchi, and A. S. Pirozhkov, "Review of laser-driven ion sources and their applications," *Reports on Progress in Physics* **75** (2012).

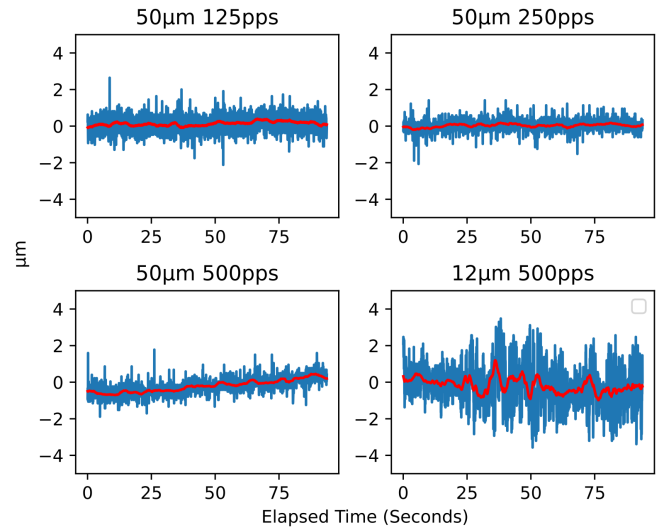


FIG. 8. Tape material positional jitter measured using the Precitec CHRcodile for different tape-drive operating speeds (125 pps to 500 pps) and two different thicknesses of Kapton tape ($12.7 \mu\text{m}$ and $50 \mu\text{m}$). As before, the blue line provides the measurement with a temporal sampling period of 15 microseconds with high frequency changes attributed to tape surface roughness. The low ($< 1 \text{ Hz}$) frequency movement, which better represents the tape motion, is shown with the red line. .

- ²E. L. Clark, K. Krushelnick, M. Zepf, F. N. Beg, M. Tatarakis, A. Machacek, M. I. K. Santala, I. Watts, P. A. Norreys, and A. E. Dangor, "Energetic heavy-ion and proton generation from ultraintense laser-plasma interactions with solids," *Phys. Rev. Lett.* **85**, 1654–1657 (2000).
- ³M. Borghesi, S. V. Bulanov, T. Z. Esirkepov, S. Fritzler, S. Kar, T. V. Li-seikina, V. Malka, F. Pegoraro, L. Romagnani, J. P. Rousseau, A. Schiavi, O. Willi, and A. V. Zayats, "Plasma ion evolution in the wake of a high-intensity ultrashort laser pulse," *Phys. Rev. Lett.* **94**, 195003 (2005).
- ⁴S. Fritzler, V. Malka, G. Grillon, J. P. Rousseau, F. Burgy, E. Lefebvre, E. d'Humières, P. McKenna, and K. W. D. Ledingham, "Proton beams generated with high-intensity lasers: Applications to medical isotope production," *Applied Physics Letters* **83** (2003).
- ⁵P. Puyuelo-Valdes, S. Vallières, M. Salvadori, S. Fourmaux, S. Payeur, J.-C. Kieffer, F. Hannachi, and P. Antici, "Combined laser-based x-ray fluorescence and particle-induced x-ray emission for versatile multi-element analysis," *Scientific Reports* **11** (2021), 10.1038/s41598-021-86657-6.
- ⁶"5-hz, 150-tw ti:sapphire laser with high spatiotemporal quality," *Journal of the Korean Physical Society* **77**, 10.3938/jkps.77.223.
- ⁷R. Lera, P. Bellido, I. Sanchez, P. Mur, M. Seimetz, J. M. Benlloch, L. Roso, and A. Ruiz-de-la Cruz, "Development of a few tw ti:sapphire laser system at 100 hz for proton acceleration," *Applied Physics B* **125** (2018), 10.1007/s00340-018-7113-8.
- ⁸Y. Gao, J. Bin, D. Haffa, C. Kreuzer, J. Hartmann, M. Speicher, F. H. Lindner, T. M. Ostermayr, P. Hilz, and T. F. e. a. Rösch, "An automated, 0.5 hz nano-foil target positioning system for intense laser plasma experiments," *High Power Laser Science and Engineering* **5** (2017), 10.1017/hpl.2017.10.
- ⁹S. Wilks, a. B. Langdon, T. E. Cowan, M. Roth, M. Singh, S. Hatchett, M. H. Key, D. Pennington, A. J. Mackinnon, and R. A. Snavely, "Energetic proton generation in ultra-intense laser–solid interactions," *Physics of Plasmas* **8**, 542 (2001).
- ¹⁰*Progression of a tape-drive targetry solution for high rep-rate HPL experiments within the CLF* (2022).
- ¹¹M. Noaman-ul Haq, H. Ahmed, T. Sokollik, L. Yu, Z. Liu, X. Yuan, F. Yuan, M. Mirzaie, X. Ge, and L. e. a. Chen, "Statistical analysis of laser driven protons using a high-repetition-rate tape drive target system," *Physical Review Accelerators and Beams* **20** (2017), 10.1103/physrevac-

celbeams.20.041301.

- ¹²M. A. Vernezi, D. V. Nazarenko, and E. H. Abderrazzak, "Vibration suppression of stepper motors by the electric method," in *2021 International Conference on Industrial Engineering, Applications and Manufacturing (ICIEAM)* (2021) pp. 566–570.
- ¹³M. Fritz and M. Groeb, "Increasing performance and energy efficiency of a machine tool through hydrostatic linear guideways with single digit micrometre fluid film thickness," *MM Science Journal* **2021**, 5241–5246 (2021).
- ¹⁴B. B. Lazan, *Damping of materials and members in structural mechanics* (Pergamon Press, 1968) p. 205.